THE FASEB JOURNAL • RESEARCH • www.fasebj.org

Dyslipidemia impairs mitochondrial trafficking and function in sensory neurons

Amy E. Rumora,*,[1] Stephen I. Lentz,†,[1] Lucy M. Hinder,* Samuel W. Jackson,* Andrew Valesano,* Gideon E. Levinson,* and Eva L. Feldman*,[2]

*Department of Neurology and †Department of Internal Medicine, University of Michigan, Ann Arbor, Michigan, USA

ABSTRACT: Mitochondrial trafficking plays a central role in dorsal root ganglion (DRG) neuronal cell survival and neurotransmission by transporting mitochondria from the neuronal cell body throughout the bundles of DRG axons. In type 2 diabetes (T2DM), dyslipidemia and hyperglycemia damage DRG neurons and induce mitochondrial dysfunction; however, the impact of free fatty acids and glucose on mitochondrial trafficking in DRG neurons remains unknown. To evaluate the impact of free fatty acids compared to hyperglycemia on mitochondrial transport, primary adult mouse DRG neuron cultures were treated with physiologic concentrations of palmitate and glucose and assessed for alterations in mitochondrial trafficking, mitochondrial membrane potential, and mitochondrial bioenergetics. Palmitate treatment significantly reduced the number of motile mitochondria in DRG axons, but physiologic concentrations of glucose did not impair mitochondrial trafficking dynamics. Palmitate-treated DRG neurons also exhibited a reduction in mitochondrial velocity, and impaired mitochondrial trafficking correlated with mitochondrial depolarization in palmitate-treated DRG neurons. Finally, we found differential bioenergetic effects of palmitate and glucose on resting and energetically challenged mitochondria in DRG neurons. Together, these results suggest that palmitate induces DRG neuron mitochondrial depolarization, inhibiting axonal mitochondrial trafficking and altering mitochondrial bioenergetic capacity.—Rumora, A. E., Lentz, S. I., Hinder, L. M., Jackson, S. W., Valesano, A., Levinson, G. E., Feldman, E. L. Dyslipidemia impairs mitochondrial trafficking and function in sensory neurons. FASEB J. 32, 195–207 (2018). www.fasebj.org

KEY WORDS: diabetic neuropathy · DRG · hyperglycemia · palmitate · mitochondrial transport

Diabetes affects ~300 million individuals worldwide, and roughly 50% of individuals with type 2 diabetes (T2DM) develop diabetic neuropathy (DN) (1–3), making DN one of the most prevalent neurologic complications. In DN, length-dependent peripheral nerve damage induces a distal-to-proximal loss of sensation, thereby causing a significant loss of individual and societal productivity (4, 5), a poor quality of life for affected individuals (1, 6, 7), and 60% of lower limb amputations (2). Glycemic control is the only current DN treatment, but clinical and experimental data show that glycemic control alone does not significantly affect DN pathogenesis in T2DM (8). More recent studies, however, have indicated that dyslipidemia correlates with progressive nerve damage and is a strong predictor of developing DN (3, 7, 9–11). Hence, understanding the cellular and molecular pathways altered by dyslipidemia is necessary to develop novel, effective therapies to prevent the onset and progression of DN.

DN is primarily a sensory neuropathy that affects dorsal root ganglion (DRG) sensory neurons that originate in the spinal cord and extend axon bundles up to 2 m in length to innervate the periphery (11). DRG neurons depend on mitochondrial glucose metabolism and fatty acid oxidation in the cell body and throughout the entire axon for ATP production (11–19); therefore, altered mitochondrial metabolism is a likely contributor to DN progression (17). Hyperglycemia and dyslipidemia both induce molecular signatures of mitochondrial dysfunction in DRG neurons, including oxidative stress and apoptosis (9–12), and, given the length-dependent damage associated with DN, it is likely that early DRG neuronal dysfunction originates in the distal DRG axon. This location potentially implicates critical mitochondrial trafficking mechanisms that transport mitochondria from the cell body throughout the DRG axon for neuronal function in DN pathogenesis; however, the impact of hyperglycemia and dyslipidemia on mitochondrial transport in DRG neurons is unknown.

ABBREVIATIONS: BSA, bovine serum albumin; Cyto b, cytochrome *b*; DN, diabetic neuropathy; DRG, dorsal root ganglion; FCCP, 4-(trifluoromethoxy)phenylhydrazone; mito-GFP, mitochondria-GFP; OCR, oxygen consumption rate; SRC, spare respiratory capacity; T2DM, type 2 diabetes; TMRM, tetramethylrhodamine methyl ester; Ywhaz, tyrosine 3-monooxygenase/tryptophan 5-monooxygenase activation protein

[1] These authors contributed equally to this work.

[2] Correspondence: Department of Neurology, University of Michigan, 5017 AAT-BSRB, 109 Zina Pitcher Place, Ann Arbor, MI 48109, USA. E-mail: efeldman@umich.edu

doi: 10.1096/fj.201700206R

This article includes supplemental data. Please visit *http://www.fasebj.org* to obtain this information.

Mitochondrial trafficking along the DRG axon is regulated by specialized mechanisms that are influenced by post-translational modifications, metabolic requirements, and intracellular calcium fluctuations (20–23). This complex process requires the motor proteins kinesin-1 and cytoplasmic dynein. Kinesin-1 facilitates anterograde mitochondrial transport away from the cell body toward the distal axon tip, whereas cytoplasmic dynein transports mitochondria retrogradely toward the cell body. These motor proteins are coupled to mitochondria *via* mitochondrial motor adaptor proteins in the Milton-Trak1/2 family and *via* the Rho GTPases Miro1 and -2 (20–25). These motor proteins and adaptors are regulated by the metabolic state of neurons. A study in rat hippocampal neurons found that elevated glucose levels regulate *O*-GlcNAcylation of Milton by *O*-GlcNAc transferase (20), thereby affecting mitochondrial transport. Moreover, metabolic regulation of calcium flux can regulate mitochondrial motility by altering the conformational state of Miro to halt mitochondrial motility. Altered mitochondrial transport is also implicated in other neurologic diseases (26–28). Therefore, in this study, we evaluated the impact of hyperglycemia and dyslipidemia on mitochondrial trafficking as a potential pathogenic mechanism for DN. We assessed specifically the effect of elevated levels of glucose and the fatty acid palmitate on mitochondrial trafficking, function, and depolarization in DRG neurons.

MATERIALS AND METHODS

Primary DRG neuron culture and treatments

Primary DRG neurons from 16- to 18-wk-old C57Bl/6J mice (The Jackson Laboratory, Bar Harbor, ME, USA) were cultured as described in several publications (11, 14, 29). In brief, cervical, lumbar, and thoracic DRGs were collected and incubated with 2 mg/ml collagenase (Millipore-Sigma, Billerica, MA, USA), dissociated in heat-inactivated fetal bovine serum, and pelleted by centrifugation to remove residual serum. Three different media were prepared as follows: treatment medium containing 50% F-12K (Cell Gro; Corning, Manassas, VA, USA), 50% DMEM (Cell Gro; Corning), 1:100 dilution of Nb^+ (13), 1000 U/ml penicillin/streptomycin/neomycin (Thermo Fisher Scientific, Waltham, MA, USA), and 7.2 μM aphidicolin (Millipore-Sigma); feed medium, containing treatment medium plus 1× B27 (Thermo Fisher Scientific); and plating medium, containing feed medium plus 2 mM L-glutamine (0.4 μM final concentration; Thermo Fisher Scientific). DRG neurons were resuspended in plating medium and transfected with CellLight mitochondria-GFP (mito-GFP; BacMam 2.0; Thermo Fisher Scientific), by adding 3.75 μl/ml mito-GFP to the dissociated DRG cells before plating in 4-well Nuc Lab-Tek chambered coverglass imaging plates (Thermo Fisher Scientific) coated with 25 μg/ml laminin (Millipore-Sigma). After 24 h, DRG neurons were switched into feed medium. After another 24 h (48 h total), primary DRG neurons had established axons and were treated with treatment medium supplemented with 25–200 mM glucose (final concentration range, 31.1–206.1 mM glucose) (Millipore-Sigma) or 31.25–250 μM palmitate for 12 or 24 h. Initial mitochondrial motility studies included a combination treatment containing both 25 mM glucose and 250 μM palmitate. For palmitate treatments, sodium palmitate (Nu-ChekPrep, Elysian, MN, USA) was conjugated to fatty acid-free bovine serum albumin (BSA) (Thermo Fisher Scientific) and diluted to treatment concentrations. Treatment medium alone was used as a control for glucose treatments, whereas 0.25% BSA was used as a control for palmitate treatments.

Mitochondrial motility and kymographing analysis

To evaluate mitochondrial trafficking in DRG neurons, we tracked the movement of individual mitochondria in live DRG neurons by time-lapse confocal microscopy (26). An A1 confocal microscope (Nikon Instruments, Melville, NY, USA) equipped with an environmental chamber (Tokai Hit, Shizuoka-ken, Japan) maintained at 5% CO_2 and 37°C was used to image DRG neurons after 12 and 24 h of treatment, using NIS Elements software (Nikon Instruments). For each live neuron, images were taken with a ×40 oil objective with the confocal aperture set for an optical thickness of 4.49 μm. The Nikon Perfect Focus system (Nikon Instruments) was used to retain focus on the sample and offset thermal drift throughout time-lapse imaging. A time series was created at ×2 zoom by recording an image every 2.5 s for 2.5 min using the NIS Elements ND acquisition to envisage the time series of confocal images.

The image time series recorded for each mito-GFP-labeled DRG neuron was quantitated with MetaMorph Software (Molecular Devices, Sunnyvale, CA, USA) (26, 30). Kymographs were generated by drawing regions of interest along the axon in the anterograde direction, from the soma toward the distal axon tip. Mitochondrial movement within 10 μm of the region of interest was recorded along the *x* axis of the kymograph, with each subsequent image of mitochondrial movement stacked downward along the *y* axis (26, 31, 32). One kymograph with average background subtraction was generated to highlight motile mitochondria, and a second kymograph with no background subtraction was generated for stationary mitochondria. Kymographs were then used to evaluate the number of motile and stationary mitochondria, the directionality of mitochondrial movement, and the velocity of motile mitochondria under each treatment or control condition with Excel (Microsoft Corp., Redmond, WA, USA). A threshold velocity, determined from the average velocity of mitochondrial movement in control conditions (26), was set at 0.02 μm/s to designate mitochondrial motility in DRG neurons (representing less than 10% of the average velocity in control conditions); therefore, mitochondria with velocities <0.02 μm/s were considered stationary. An average of 15 neurons from 3 to 5 separate experimental replicates were analyzed for each treatment condition.

Mitochondrial membrane potential analysis

Mitochondrial polarization state was assessed with tetramethylrhodamine methyl ester (TMRM) (Thermo Fisher Scientific) (18, 29, 33). TMRM is a cationic fluorophore that sequesters to the matrix of polarized mitochondria but diffuses upon mitochondrial depolarization (34). Primary DRG neurons transfected with mito-GFP were cultured as described above for 48 h to establish axons, treated with glucose or palmitate for 24 h, and incubated in the respective treatment plus 50 nM TMRM for 30 min at 37°C. After TMRM staining, the respective TMRM-containing treatment was removed, DRG neuron cultures were washed twice with treatment medium, and the respective treatments without TMRM were replaced. Live-cell confocal microscopy was used to take single, sequential images of mito-GFP (green channel) and TMRM costaining (red channel) in DRG neurons with a ×40 oil objective. TMRM staining intensity was analyzed by creating a threshold intensity level with the MetaMorph Image Analysis program (Molecular Devices). All data acquired from MetaMorph were then analyzed by detecting the fluorescence intensity of TMRM signal masked to mito-GFP-labeled

mitochondria, to differentiate between polarized and depolarized mitochondria. TMRM signals below 1000 intensity units (1.5% max, range 0–65,536) were considered depolarized. An average of 51 neurons from 3 to 5 separate experimental replicates were analyzed for each treatment condition.

Mitochondrial bioenergetic profiling

Mitochondrial bioenergetic function in treated and control DRG cultures was evaluated with an XF24 Extracellular Flux Analyzer (Agilent Technologies, Santa Clara, CA, USA) (35). DRG neurons harvested from two 16- to 18-wk-old mice were cultured in a laminin-coated 24-well Seahorse plate (Seahorse Bioscience, Chicopee, MA, USA) as above. After 48 h, DRG neurons had established axons, and cultures were treated with 100 mM glucose or 62.5–250 μM palmitate for 24 h. Cultures were changed into buffer-free DMEM [supplemented with 1 mM sodium pyruvate, 6.27 mM D-glucose, and 3 mM Glutamax (pH 7.4); Thermo Fisher Scientific] 1 h before mitochondrial respiration measurements. For bioenergetic profiling, stable baseline oxygen consumption rate (OCR) measurements were established for resting DRG neurons, followed by measurements of real-time OCR subsequent to sequential injection of 1.25 μM oligomycin, 300–1000 nM carbonyl cyanide-4-(trifluoromethoxy)phenylhydrazone (FCCP), and 1 μM antimycin A (all from Millipore-Sigma). The dose-response of the uncoupling protonophore FCCP measured changes in mitochondrial respiration metrics in challenged DRG neurons. These metrics were then used to evaluate the spare respiratory capacity (SRC), an assessment of the ability of treated DRG neurons to produce excess ATP by oxidative phosphorylation under increased energy demand. Oligomycin and antimycin A inhibited oxidative phosphorylation for derivation of ATP-linked mitochondrial respiration and nonmitochondrial respiration parameters. The number of plates per condition was 7 for treatment medium, 4 for 0.25% BSA, and 2 for all other conditions. Bioenergetic parameters were derived from response curves, normalized to total protein concentration, and reported as a mean of all repetitions (36).

Mitochondrial copy number analysis

Primary DRG neurons from four 16- to 18-wk-old mice were cultured in a 24-well laminin-coated cell culture plate as described above for 48 h. DRG neurons were then treated in triplicate with treatment medium and 0.25% BSA, 62.5–250 μM palmitate, or 50–100 mM glucose. After 24 h, DNA was isolated from DRG neuron cultures by using the AllPrep DNA/RNA Mini Kit (Qiagen, Germantown, MD, USA). Mitochondrial copy number was determined for each treatment condition by comparing the expression of mitochondria-encoded cytochrome *b* (*cyto b*) to nuclear-encoded tyrosine 3-monooxygenase/tryptophan 5-monooxygenase activation protein (*Ywhaz*): forward primer: 5′-AAGACAGCACGACGCTAATAATGC-3′ and reverse primer: 5′-TTGGAAGGCCGGTTAATTTTC-3′. Gene expression was calculated by the standard curve method with sequence-specific primers and Power SYBR Green PCR Master Mix on a StepOnePlus Real-Time PCR System (both from Thermo Fisher Scientific).

Statistical analyses

Statistical analysis of mitochondrial trafficking, mitochondrial bioenergetic parameters, and mitochondrial depolarization data was performed with Prism, v.6 (GraphPad Software, La Jolla, CA, USA), and results are presented as means ± SEM. One-way ANOVA with Tukey's *post hoc* test for multiple comparisons was performed for mitochondrial trafficking and mitochondrial depolarization data. For mitochondrial bioenergetics, treatment medium/glucose and BSA/palmitate were considered separate groups; resting metrics were evaluated with 1-way ANOVA with Tukey's *post hoc* test for multiple comparisons, and challenged metrics were analyzed with 2-way ANOVA performed on 2 datasets at a time, with the Bonferroni *post hoc* test for multiple comparisons between FCCP concentrations (37). Mitochondrial trafficking and depolarization data were statistically significant at $P < 0.01$ and bioenergetic parameters at $P < 0.05$.

RESULTS

Palmitate reduces the percentage of motile mitochondria

To evaluate the impact of extracellular glucose and palmitate on mitochondrial motility in sensory neurons, we tracked mitochondrial movement in live DRG neurons expressing mito-GFP with time-lapse confocal microscopy and developed kymographs (**Fig. 1*A***). In the treatment medium and 0.25% BSA control conditions containing normal physiologic levels of glucose (6.1 mM glucose), ~40% of mitochondria were motile. The physiologic blood glucose and saturated fatty acid levels of a diabetic patient (33–35) were then modeled by treating DRG neurons with 50 mM glucose, 250 μM palmitate, or a combination of both 25 mM glucose and 250 μM palmitate. Although 50 mM glucose alone did not alter the percentage of motile mitochondria, with ~40% motile mitochondria similar to controls, 250 μM palmitate reduced mitochondrial transport after 12 h of treatment and nearly abolished mitochondrial movement by 24 h (Fig. 1*B*, *C*). DRG neurons treated with the 25 mM glucose/250 μM palmitate combination exhibited a reduction in mitochondrial trafficking similar to that of 250 μM palmitate (Fig. 1*B*, *C*). These results suggest that physiologic palmitate levels have an inhibitory effect on mitochondrial trafficking.

To gain further insight into the effect of hyperglycemia and dyslipidemia on mitochondrial motility in DRG neurons, we next evaluated the overall motile mitochondria percentages at 12 and 24 h after treatment with a range of glucose and palmitate concentrations. At both time points, 50–200 mM glucose did not reduce the percentage of motile mitochondria (**Fig. 2*A*, *C*, *E***), whereas 50 mM glucose appeared to trigger a slight but significant increase in the number of motile mitochondria at 12 h only (Fig. 2*C*). These data indicate that physiologic glucose increases alone do not alter the percentage of motile mitochondria in DRG neurons. Treatment with physiologic diabetic palmitate concentrations ranging from 62.5 to 250 μM, on the other hand, induced a significant, dose-dependent reduction in motile mitochondria percentages after 12 h (Fig. 2*B*, *D*), and motile mitochondria were nearly abolished in the presence of 125 and 250 μM palmitate after 24 h (Fig. 2*B*, *F*). The 31.25 μM palmitate treatment did not significantly decrease mitochondrial motility at either time

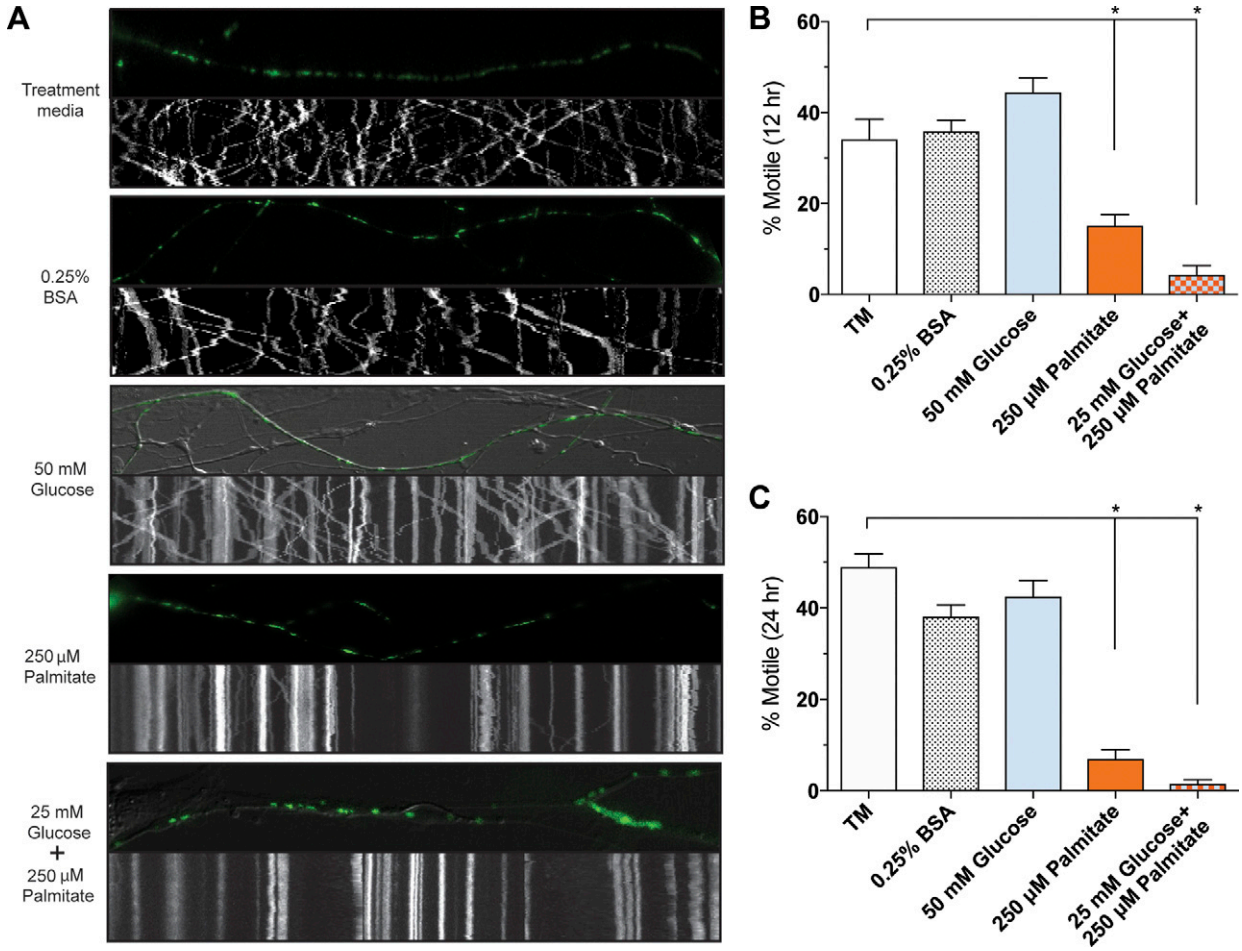

Figure 1. Diabetic physiologic concentrations of palmitate inhibit mitochondrial transport in mouse DRG neurons. *A*) Kymographs of mitochondrial motility in DRG axons expressing mito-GFP treated with treatment medium (TM), 0.25% BSA, 50 mM glucose, 250 µM palmitate, and 25 mM glucose+250 µM palmitate. The top panel of each kymograph is a representative image of the axon from the 2.5-min time series that was used to develop the corresponding kymograph. *B*, *C*) The percentage of motile mitochondria in each treatment condition after 12 h (*B*) or 24 h (*C*) of treatment. Values are expressed as means ± SEM. $^*P < 0.01$, ordinary 1-way ANOVA with Tukey's multiple-comparisons test.

point after treatment (Fig. 2*B, D, F*), suggesting that DRG neurons metabolize low palmitate levels without altering mitochondrial trafficking dynamics.

Mitochondrial trafficking directionality is not altered by glucose or palmitate

Given that neuronal mitochondrial movement is bidirectional (21), we next determined whether glucose or palmitate alters anterograde or retrograde mitochondrial transport. After 24 h of glucose or palmitate treatment, there were no significant differences in overall mitochondrial directionality relative to the treatment media and 0.25% BSA controls in the anterograde direction (**Fig. 3*A, B***). Similarly, treatment with any glucose or palmitate concentration did not induce significant alterations in the number of mitochondria moving in the retrograde direction (Fig. 3*C, D*). At 12 h of treatment, DRG neurons exhibited bidirectional mitochondrial movement similar to that seen after 24 h (Supplemental Fig. 1), indicating that there is no time-dependent change in mitochondrial directionality. Together, these results suggest that inhibition of mitochondrial trafficking by elevated glucose or palmitate does not alter the directionality of mitochondrial movement.

Palmitate alters mitochondrial trafficking velocity

Because the percentage of motile mitochondria is altered under physiologic palmitate concentrations, we next assessed the impact of glucose and palmitate on mitochondrial velocity. After 24 h of treatment, there were no significant reductions in anterograde or retrograde velocity in DRG neurons treated with 50–200 mM glucose (**Fig. 4*A, C***). With 62.5–250 µM palmitate, however, there was a significant decrease in anterograde velocity (Fig. 4*B*) as well as a trending reduction in retrograde velocity (Fig. 4*D*). Of note, similar effects were apparent after 12 h of treatment: there was a significant increase in anterograde velocity at 50 mM glucose, and palmitate induced a decrease in retrograde velocity at 62.5 and 250 µM palmitate (Supplemental Fig. 2).

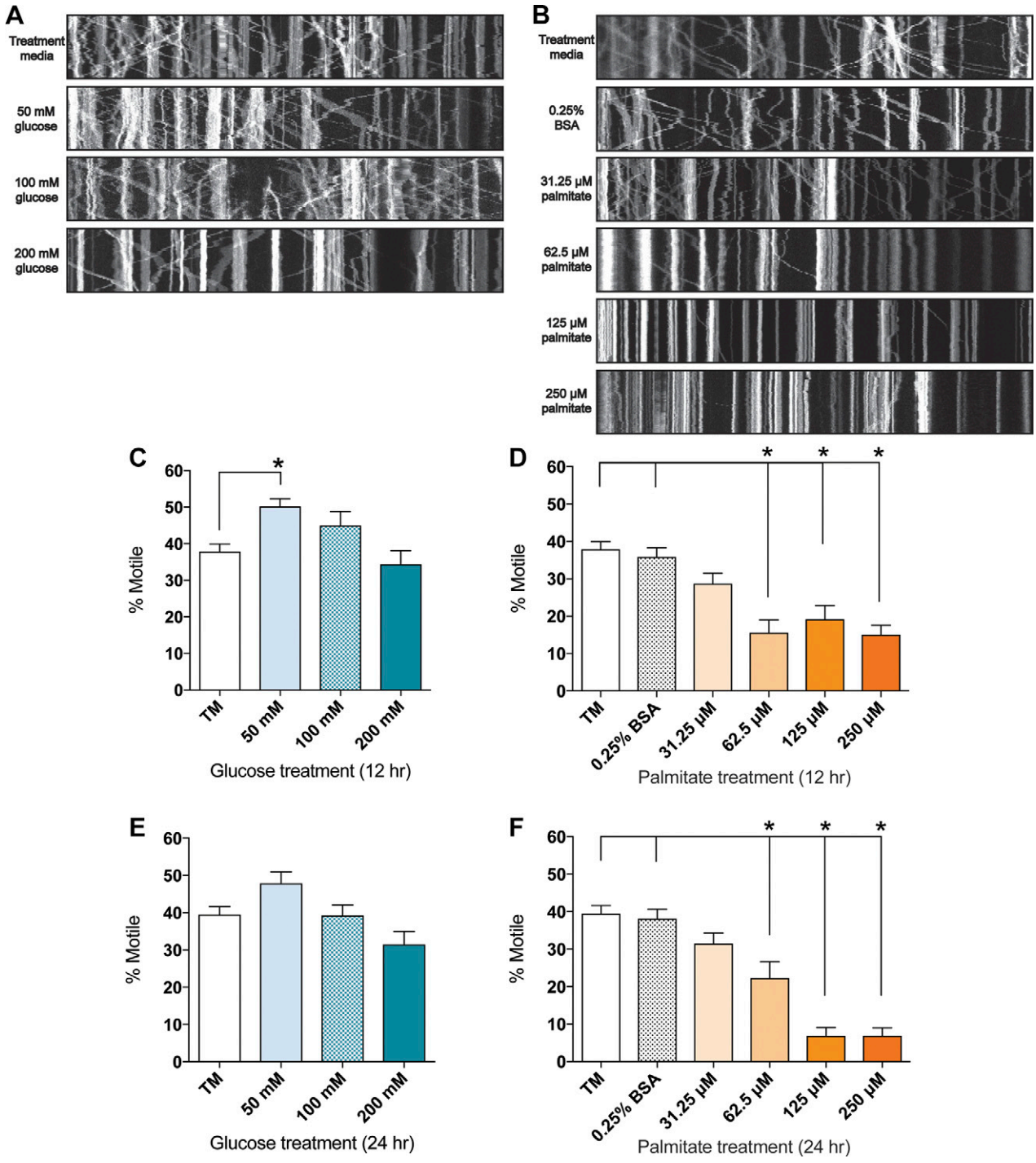

Figure 2. Elevated palmitate induces a dose-dependent decrease in mitochondrial trafficking in mouse DRG neurons. *A*, *B*) Changes in the number of motile mitochondria visible in kymographs of mitochondrial motility in DRG axons treated for 24 h with 50–200 mM glucose (*A*) or 31.25–250 μM palmitate (*B*). Each panel depicts a representative kymograph from the 2.5-min time series. *C–F*) The average percentage of motile mitochondria after treatment with 50–200 mM glucose (*C*, *E*) or 31.25–250 μM palmitate (*D*, *F*), as quantitated using the kymograph analysis. The percentage of motile mitochondria was assessed after 12 h (*C*, *D*) and 24 h (*E*, *F*). Values are expressed as means ± SEM. $^*P < 0.01$, ordinary 1-way ANOVA with Tukey's multiple-comparisons test.

Palmitate-induced mitochondrial depolarization is associated with altered trafficking dynamics

Mitochondrial uncoupling results in depolarization of the mitochondrial membrane and consequent detachment of mitochondrial molecular motors from the microtubule, resulting in impaired mitochondrial motility (38–41). Therefore, we used TMRM staining to examine the impact of glucose and palmitate on mitochondrial depolarization in DRG neurons as a potential mechanism for palmitate-induced inhibition of mitochondrial

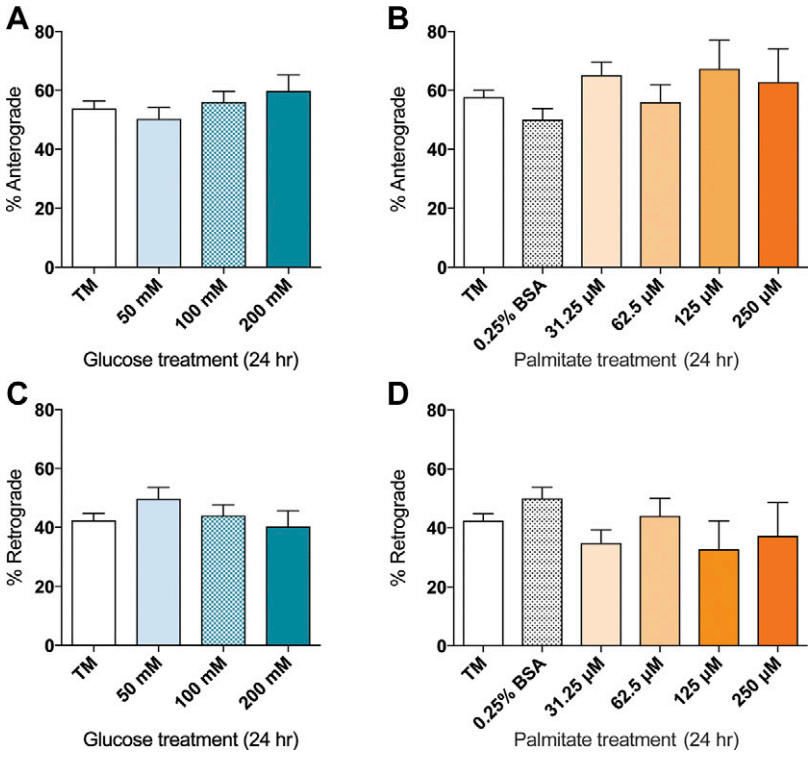

Figure 3. Effect of glucose and palmitate treatments on directionality of mitochondrial transport. No significant alteration in directionality of trafficking was observed after 24 h of 50–200 mM glucose treatments (*A*, *C*) or 31.25–250 μM palmitate treatments (*B*, *D*) in the anterograde (*A*, *B*) or retrograde (*C*, *D*) direction. Values are expressed as means ± SEM. $*P < 0.01$, ordinary 1-way ANOVA with Tukey's multiple comparisons test.

trafficking (19, 29). Punctate TMRM staining in DRG neurons treated with control medium and 0.25% BSA confirmed that mitochondria in control culture conditions retained mitochondrial membrane polarization (**Fig. 5*A–C, G***). Glucose (100 mM) did not affect the mitochondrial membrane potential, showing no change in the percentage of depolarized mitochondria (Fig. 5*G*). DRG neurons treated with 62.5–250 μM palmitate, however, exhibited a significant dose-dependent increase in mitochondrial depolarization (Fig. 5*G*) which was discernible in the diffusely stained axonal mitochondria (Fig. 5*D–F*) and reflected in the dose-dependent decrease in mitochondrial trafficking.

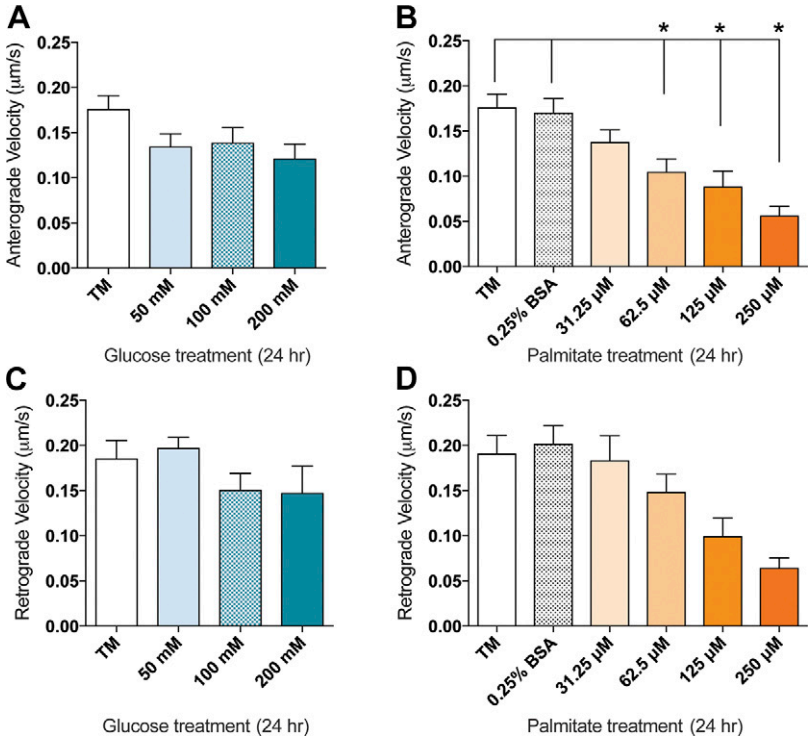

Figure 4. Dose-dependent reduction in mitochondrial trafficking velocity in glucose- and palmitate-treated mouse DRG neurons. A significant reduction in anterograde mitochondrial trafficking velocity was visible after 24 h of treatment with palmitate (*B*) concentrations that inhibit mitochondrial trafficking. Similarly, a trending reduction in retrograde mitochondrial trafficking velocity was visible after 24 h of treatment with elevated concentrations of palmitate (*D*). No significant differences in anterograde (*A*) or retrograde (*C*) mitochondrial trafficking velocity were evident after 24 h of 50–200 mM glucose treatment. Values are expressed as means ± SEM. $*P < 0.01$, ordinary 1-way ANOVA with Tukey's multiple-comparisons test.

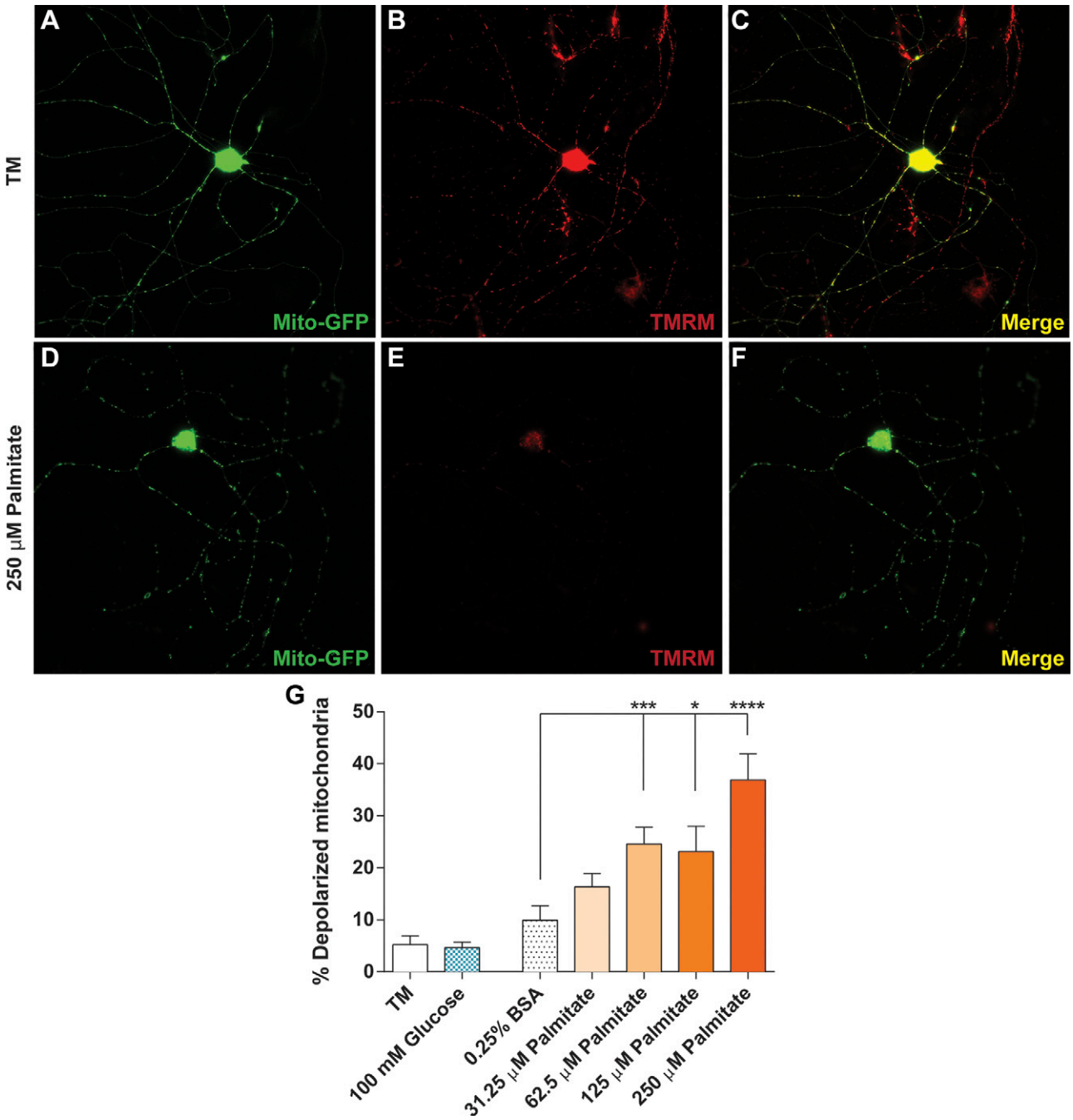

Figure 5. Elevated palmitate treatments induce mitochondrial depolarization. *A–C*) DRG neurons expressing mito-GFP (*A*) treated with control treatment medium (TM) retained mitochondrial polarization, as depicted by punctate TMRM staining (*B*). Polarized mitochondria appear yellow in an overlay of mito-GFP (green) and TMRM (red) signal (*C*). *D–F*) Mitochondria in DRG neurons labeled with mito-GFP (*D*) and treated with 250 μM palmitate exhibited decreases in TMRM staining (*E*) because of mitochondrial depolarization. When the mito-GFP (green) and TMRM (red) channels are merged, depolarized mitochondria appear green because of diffuse TMRM staining (*F*). *G*) DRG neurons treated with 62.5–250 μM palmitate exhibited a significant, dose-dependent increase in the number of depolarized mitochondria relative to the 0.25% BSA, TM, and 100 mM glucose-treated cells. Values are expressed as means ± SEM. $^*P < 0.01$, ordinary 1-way ANOVA with Tukey's multiple-comparisons test.

Palmitate induces a dose-dependent reduction in DRG neuron bioenergetic capacity

To assess the impact of hyperglycemia and dyslipidemia on mitochondrial function, we evaluated the bioenergetic parameters of DRG neurons treated with elevated glucose and palmitate at rest or after energetically challenging them with the mitochondrial uncoupler, FCCP. In the resting state, DRG neurons displayed a decrease in mitochondrial respiration and ATP production at 100 mM glucose, as well as a decrease in proton leak compared to

the treatment medium control (**Fig. 6*A–D***). The coupling efficiency was maintained in 100 mM glucose-treated DRG neurons, with ~80% of the oxygen consumed by the mitochondria coupled to ATP production (Fig. 6*C*). A significant reduction in both absolute and relative SRC was observed for 100 mM glucose-treated neurons (Fig. 6*E, F*). These treatments also induced a lower OCR, diminished the dose-dependent effect of FCCP, and nearly abolished aerobic respiration. These data suggest that elevated glucose concentrations induce a reduction in mitochondrial respiration in resting and challenged DRG neurons.

We next evaluated the bioenergetic parameters of DRG neurons treated with 62.5–250 μM palmitate. Because there were no differences in bioenergetics between the treatment medium and the 0.25% BSA vehicle controls, we compared all palmitate-induced bioenergetic changes to the 0.25% BSA control. Although DRG neurons treated with 62.5 μM palmitate exhibited normal resting and challenged mitochondrial bioenergetics comparable to 0.25% BSA (Fig. 6*A–D, G, H*), DRG neurons treated with 125 μM palmitate revealed increased basal respiration and ATP turnover while maintaining coupling efficiency. This increase in resting bioenergetic parameters resulted in a proportional increase in proton leak, with 70% of oxygen expenditure coupled to ATP production (Fig. 6*A–D*). DRG neurons treated with 250 μM palmitate maintained increased resting mitochondrial respiration and ATP production and also revealed reduced coupling efficiency and increased proton leak, reducing the coupling efficiency to ~65% (Fig. 6*A–D*). Moreover, palmitate-treated DRG neurons challenged with FCCP exhibited increased absolute SRC at lower palmitate concentrations, but decreased absolute SRC at 250 μM palmitate (Fig. 6*G*). Relative SRC measurements, which account for basal respiration changes, revealed that 125 and 250 μM palmitate diminished the FCCP dose-response, resulting in a 25 and 69% decrease in SRC, respectively, whereas 62.5 μM palmitate increased SRC similar to the 0.25% BSA control (Fig. 6*H*). Overall, these results suggest that mild uncoupling is a compensatory mechanism for adapting to slight increases in palmitate substrate availability; however, DRG neuronal mitochondria fail to maintain efficient energy production to match further increases in palmitate concentration. Thus, these data indicate that glucose and fatty acids have differential effects on mitochondrial bioenergetics.

Finally, because mitochondrial biogenesis varies with metabolic flux to maintain energetic homeostasis, we examined how the glucose and palmitate treatment effects on mitochondrial bioenergetics correlate with mitochondrial copy number. DRG neurons exhibited a significant increase in mitochondrial copy number in the presence of 50–100 mM glucose, whereas mitochondrial copy number was maintained after treatment with 62.5–125 μM palmitate and increased only at 250 μM palmitate (Fig. 6*I*). These results suggest that DRG neurons exhibiting reduced SRC under high glucose and palmitate treatments may undergo biogenesis in an attempt to compensate for excess substrate availability and enhance SRC by increasing the mitochondrial copy number (42).

DISCUSSION

Neurons depend on mitochondrial trafficking mechanisms to distribute mitochondria throughout axons (43–48); however, the impact of altered diabetic concentrations of glucose or fatty acids on mitochondrial trafficking in DRG neurons is unknown. We assessed the effect of extracellular glucose and palmitate on mitochondrial trafficking and mitochondrial function in primary DRG neurons and found that physiologic glucose levels did not alter mitochondrial movement or mitochondrial membrane potential, but significantly diminished mitochondrial respiration and increased biogenesis. Physiologic concentrations of palmitate, on the other hand, significantly impaired axonal mitochondrial motility and velocity in DRG neurons in a dose-dependent manner that correlated with impaired mitochondrial energy production, increased mitochondrial copy number, and a higher percentage of depolarized mitochondria. These data suggest that excess palmitate, but not glucose, impairs mitochondrial transport throughout the axon in DRG neurons *in vitro* and could provide a rationale for clinical studies elucidating a central role for dyslipidemia in sensory neuron cell damage and DN development (3, 7–11).

Diabetes is diagnosed when circulating blood glucose levels are >11 mM, whereas levels in a healthy individual typically fall between 4 and 6.1 mM (49). Likewise, the level of serum glucose in diabetic rats (40.1 ± 1.9 mM) is 2.5–3 times higher than the level of glucose in the sciatic nerve (16.2 ± 0.7 mM/kg wet weight) (50). Therefore, to mimic normoglycemic conditions, our DRG neuron culture medium contains 6.1 mM glucose. To model physiologic hyperglycemic concentrations, we initially used 25–50 mM added glucose (Fig. 1) and then increased treatment concentrations up to 200 mM added glucose to evaluate the impact of increased glucose levels on mitochondrial trafficking (Fig. 2). To assess how dyslipidemia affects mitochondrial motility, we used palmitate, a 16-carbon saturated fatty acid that serves as a biomarker for T2DM and constitutes 30% of nonesterified fatty acids in human plasma (51). Although fatty acid concentration fluctuates based on diet, a recent study measuring the human serum metabolome observed 66–125 μM palmitate (52), whereas another study measuring serum palmitate in healthy mice found levels up to 250 μM (53). Hence, diabetic mice would be likely to exhibit physiologic concentrations of palmitate up to 250 μM or higher. Thus, to evaluate the impact of dyslipidemia on mitochondrial transport in DRG axons, we used physiologically relevant palmitate concentrations between 31.25–250 μM (54–56). We found that 50–200 mM extracellular glucose had no impact on mitochondrial motility, whereas 62.5–250 μM palmitate arrested mitochondrial movement in DRG neurons.

Although physiologic glucose levels did not affect mitochondrial movement in DRG neurons, physiologic palmitate concentrations nearly abolished mitochondrial trafficking. These findings contrast with those in a recent study that identified a connection between glucose metabolism and post-translational modification of the

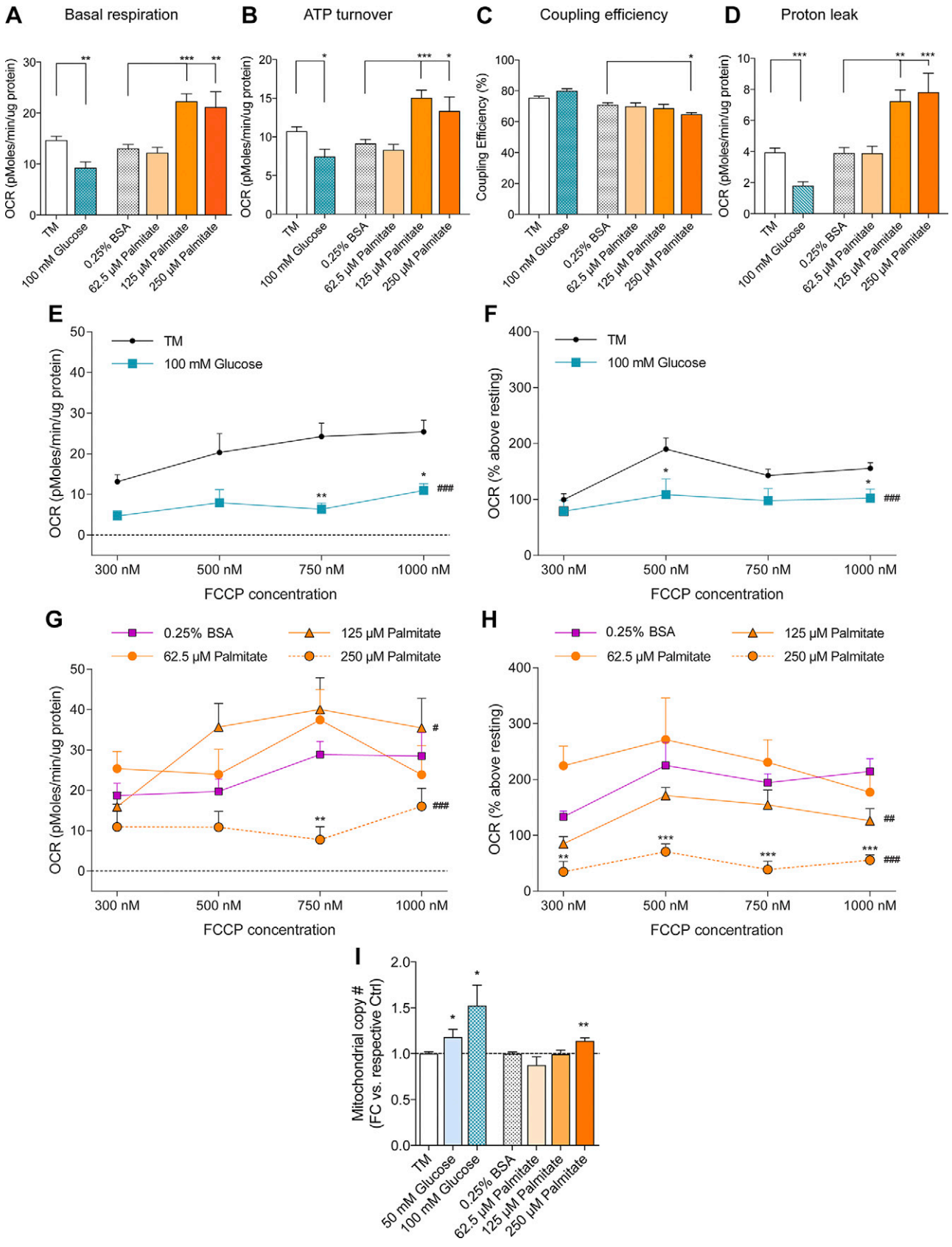

Figure 6. Glucose and palmitate induce differential mitochondrial respiratory phenotypes in DRG neurons. After stable baseline OCR measurements, mitochondrial bioenergetic profiles were determined by sequential addition of oligomycin (ATP-synthase inhibitor), FCCP [carbonyl cyanide-4-(trifluoromethoxy)phenylhydrazone, uncoupler], and antimycin A (complex III inhibitor) for final concentrations of 1.25 µM, 300–1000 nM, and 1 µM, respectively. *A–D*) Resting

(*continued on next page*)

mitochondrial motor protein Milton that resulted in impaired mitochondrial trafficking in primary rat hippocampal neurons (20). Specifically, the metabolic sensor *O*-GlcNAc transferase prompted GlcNAcylation of Milton under elevated glucose concentrations (57). This glucose-mediated regulation of mitochondrial trafficking in hippocampal neurons highlights the impact of metabolic flux on mitochondrial trafficking (58); however, the divergence between this glucose-mediated reduction in mitochondrial trafficking and our data examining fatty acid-mediated impairment of mitochondrial transport suggest that regulatory factors controlling mitochondrial trafficking dynamics in peripheral DRG neurons are unique from those in central nervous system hippocampal neurons. Therefore, palmitate may impair mitochondrial movement in DRG neurons by a unique regulatory mechanism.

Bidirectional mitochondrial movement is fundamental to neuronal health; however, exogenous or endogenous factors can alter the directionality of mitochondrial movement, resulting in a bias toward anterograde or retrograde movement. Across all glucose and palmitate treatment conditions, the motile mitochondria in DRG neurons maintained bidirectional movement, despite a dose-dependent decrease in velocity (Figs. 3 and 4). These results suggest that elevated glucose concentrations do not impair neuronal mitochondrial directionality, and may target dysfunctional mitochondria to the cell body for degradation (39, 59, 60). In addition, the maintained bidirectional mitochondrial movement across glucose and palmitate concentrations suggests that a preference for retrograde movement is not necessary to transport damaged mitochondria to the cell body for degradation (44, 59, 61, 62). Instead, a steady decrease in mitochondrial velocity paralleling an overall reduction in the percentage of motile mitochondria is suggestive of global mitochondrial dysfunction (42, 63). The reduction in mitochondrial trafficking with no bias toward retrograde or anterograde directionality points to molecular changes in mitochondrial adaptor proteins that attach mitochondria to anterograde-directed kinesin-1 or retrograde moving dynein. The GTPase family of mitochondrial adaptors, Miro1 and -2, has been identified as neuronal calcium sensors (64, 65). Miro mitochondrial adaptors undergo structural changes upon binding calcium in response to elevated levels of intracellular calcium flux. This conformational change facilitates detachment of the mitochondria from molecular motors, thereby halting mitochondrial trafficking. Calcium dysregulation associated with palmitate (66) may therefore be responsible for impaired mitochondrial trafficking in hyperlipidemic DRG neurons, and this palmitate-induced calcium dyshomeostasis could occur by direct or indirect mechanisms (67). Palmitate has been shown to form direct interactions with calcium channels to trigger elevation in intracellular calcium levels (65, 68, 69). Alternatively, palmitate can also induce increases in intracellular calcium indirectly by activating G-protein-coupled receptor 40 (70, 71). Other potential mechanisms that could impair mitochondrial motility include changes affecting anchoring proteins or post-translational modifications that inhibit mitochondrial movement (46). Irrespective of the molecular mechanism underlying metabolically dysregulated mitochondrial trafficking, the resulting energetic dysregulation and mitochondrial dysfunction may contribute to neuronal dysfunction.

Given that mitochondrial membrane depolarization has been implicated in arrested mitochondrial trafficking in neurons and ultimately results in reduced bioenergetic capacity, which may play a significant role in neuronal dysfunction (39, 41), we next evaluated the impact of glucose and palmitate on mitochondrial depolarization. Although glucose did not significantly affect mitochondrial membrane polarization in adult DRG neurons, palmitate treatment induced mitochondrial depolarization (Fig. 5). There is a clear role for palmitate in mitochondrial depolarization in many cell lineages (72–74); however, the contribution of glucose in mitochondrial depolarization of DRG neurons remains disputable (75). Studies in embryonic DRG neurons indicate that 45 mM glucose induces oxidative stress and mitochondrial dysfunction (15, 16, 18), whereas adult rat DRG neurons treated with up to 60 mM glucose exhibited no significant increase in neuronal oxidative stress or cell death (76, 77). This discrepancy could be due to differing nutrient requirements and physiologic states of embryonic compared to adult DRG neurons (78). Our results, however, show that glucose concentrations exceeding physiologic levels do not significantly alter mitochondrial depolarization, suggesting that primary DRG neurons from adult mice are resistant to glucose-induced mitochondrial depolarization. Palmitate, on the other hand, induced significant mitochondrial membrane depolarization. Therefore, we contend that dyslipidemia and hyperglycemia in adult DRG neurons is the most accurate model of sensory neuronal changes *in vivo* (75).

We next evaluated the impact of glucose and palmitate on mitochondrial bioenergetics as a marker of mitochondrial function. These bioenergetic studies indicated that elevated glucose concentrations significantly altered the resting bioenergetic state of DRG neurons, as indicated by a reduction in mitochondrial respiration, compromised ATP turnover, proton leak, and mitochondrial uncoupling (Fig. 6*A–D*). Furthermore, challenged DRG neurons exhibited an even greater reduction in glucose-induced mitochondrial respiration (Fig. 6*E, F*). The decrease in mitochondrial oxygen consumption suggests that elevated levels of glucose compromise the mitochondrial

mitochondrial bioenergetic phenotype. *E–H*) Absolute SRC (*E*, *G*), and SRC expressed as a percentage of resting basal respiration determined in *A*, *F*, and *H*. *I*) Mitochondrial copy number was assessed by normalizing mitochondrial gene expression (*cyto b*) to nuclear gene expression [tyrosine 3-monooxygenase/tryptophan 5-monooxygenase activation protein (*Ywhaz*)]. Data are expressed as fold-change (FC) in copy number relative to respective control. $^{*}P < 0.05$, $^{**}P < 0.01$, $^{***}P < 0.001$ *vs.* respective control, 1-way ANOVA with Tukey's multiple-comparisons test (*A–D*, *I*) or Bonferroni multiple-comparisons *post hoc* text (*E–H*); $^{\#}P < 0.05$, $^{\#\#}P < 0.01$, $^{\#\#\#}P < 0.001$, 2-way ANOVA whole-curve effect of treatment *vs.* control. Values are expressed as means ± SEM.

respiratory chain in DRG neurons but have no effect on mitochondrial membrane polarization. These results differ from those of previous studies showing that hyperglycemia leads to programmed cell death, decreased uncoupling protein expression, and induction of mitochondrial depolarization in embryonic DRG neurons (79); however, the current data support previous studies showing diminished mitochondrial respiratory activity in STZ-treated rats and reduced mitochondrial glucose oxidation in the peripheral nerves of *db/db* mice (35, 80). Overall, the current data show that hyperglycemia reduces mitochondrial respiration in concert with increases in mitochondrial copy number in DRG neurons from adult mice, suggesting that mitochondrial biogenesis is a compensatory mechanism to adapt to increased glucose (81).

The current study further revealed that excess glucose and palmitate induced differential effects on mitochondrial bioenergetics. DRG neurons treated with 62.5 μM palmitate exhibited normal mitochondrial respiration under both resting and challenged conditions, and mitochondrial copy number was also maintained, even when palmitate induced mitochondrial membrane depolarization. Concentrations of 125 and 250 μM palmitate increased resting ATP production and basal respiration, but corresponded with mitochondrial proton leak (Fig. 6*A–D*). ATP production was unaffected by the mild uncoupling effect observed under the highest palmitate treatment, suggesting that slight mitochondrial uncoupling represents a compensatory mechanism to limit generation of reactive oxygen species (82). Although energy production is maintained under palmitate treatment, increasing palmitate concentrations impaired oxidative phosphorylation during high energy demand, limiting the ability of neuronal mitochondria to achieve the energy production necessary to maintain mitochondrial trafficking and respiratory chain capacity. Overall, the mitochondrial depolarization and impaired trafficking at 62.5–250 μM palmitate suggests that, although mitochondria maintain normal function, elevated palmitate impairs mitochondrial trafficking which may prevent distribution of mitochondria throughout the axon where ATP is required for neuronal function.

Together, the results presented herein draw a correlation between palmitate-induced mitochondrial depolarization, altered bioenergetic function, and impaired mitochondrial trafficking in DRG neurons. To our knowledge, this is the first study linking fatty acid-induced mitochondrial depolarization to a reduction in mitochondrial motility. This observation is supported by studies identifying chemical mitochondrial uncouplers that induce mitochondrial depolarization and halt mitochondrial trafficking (38–41), indicating that ATP production and mitochondrial polarization are closely linked. Our studies also depict differential effects of glucose and palmitate on mitochondrial bioenergetic parameters. Although glucose severely diminishes mitochondrial respiration, palmitate reduces mitochondrial trafficking and mitochondrial membrane polarization without impacting mitochondrial biogenesis or bioenergetics. These differential effects of glucose and palmitate on mitochondrial trafficking dynamics and bioenergetics may provide a rationale for the correlation between dyslipidemia and progressive nerve damage, as glycemic control remains an ineffective treatment for DN in T2DM (83). The collective results of our study delineate distinctive effects of glucose and fatty acids on mitochondrial dynamics, providing novel evidence of palmitate-induced alterations of mitochondrial bioenergetics, mitochondrial membrane polarization, and mitochondrial axonal trafficking mechanisms. FJ

ACKNOWLEDGMENTS

The authors thank Dr. Stacey Sakowski Jacoby for expert editorial advice; Carey Backus for lending expertise in mitoDNA quantitative PCR analyses; and John M. Hayes, Colin M. Mervak, and Nandini S. Abburi (all from the University of Michigan) for contributions to pilot trafficking and mitochondrial depolarization experiments. Funding was provided by U.S. National Institutes of Health (NIH) National Institute of Diabetes and Digestive and Kidney Diseases (NIDDK) Grants R24 DK082841 and R01 DK107956 (to E.L.F.) and T32 1T32DK101357-01 (to A.E.R.); Novo Nordisk Foundation Grant NNF14SA0006 (to E.L.F.); Juvenile Diabetes Research Foundation's Angelika Bierhaus Postdoctoral Fellowship in Diabetic Complications (to L.M.H.); American Diabetes Association, Program for Neurology Research and Discovery; and the A. Alfred Taubman Medical Research Institute. Confocal microscopy and image analysis were performed with equipment at the Michigan Diabetes Research Center's Microscopy and Image Analysis Core, supported by NIH, NIDDK Grant P60DK020572; and University of Michigan Core Services, supported by NIH NIDDK Grant DK089503 (Seahorse XF Analyzer). A.E.R. and S.I.L. share senior authorship. The authors declare no conflicts of interest.

AUTHOR CONTRIBUTIONS

A. E. Rumora, S. I. Lentz, and L. M. Hinder designed the research; A. E. Rumora, L. M. Hinder, S. W. Jackson, A. Valesano, G. E. Levinson analyzed the data; A. E. Rumora, L. M. Hinder, S. W. Jackson, and A. Valesano performed the research; A. E. Rumora and L. M. Hinder wrote the paper; S. I. Lentz developed the kymograph and TMRM image analysis programs necessary to analyze mitochondrial trafficking experiments and TMRM depolarization experiments, respectively; and E. L. Feldman directed the study, provided scientific expertise, and reviewed the manuscript.

REFERENCES

1. Centers for Disease Control and Prevention. (2014) *National Diabetes Statistics Report: Estimates of Diabetes and Its Burden in the United States*, U.S. Department of Health and Human Services, Atlanta, GA, USA
2. International Diabetes Federation (IDF). (2015) *IDF Diabetes Atlas*, 7th ed., IDF, Brussels, Belgium
3. Young, M. J., Boulton, A. J., MacLeod, A. F., Williams, D. R., and Sonksen, P. H. (1993) A multicentre study of the prevalence of diabetic peripheral neuropathy in the United Kingdom hospital clinic population. *Diabetologia* **36**, 150–154
4. Edwards, J. L., Vincent, A. M., Cheng, H. T., and Feldman, E. L. (2008) Diabetic neuropathy: mechanisms to management. *Pharmacol. Ther.* **120**, 1–34
5. Breton, M. C., Guénette, L., Amiche, M. A., Kayibanda, J. F., Grégoire, J. P., and Moisan, J. (2013) Burden of diabetes on the ability to work: a systematic review. *Diabetes Care* **36**, 740–749

6. Callaghan, B. C., Cheng, H. T., Stables, C. L., Smith, A. L., and Feldman, E. L. (2012) Diabetic neuropathy: clinical manifestations and current treatments. *Lancet Neurol.* **11**, 521–534
7. Boulton, A. J., Vinik, A. I., Arezzo, J. C., Bril, V., Feldman, E. L., Freeman, R., Malik, R. A., Maser, R. E., Sosenko, J. M., and Ziegler, D.; American Diabetes Association. (2005) Diabetic neuropathies: a statement by the American diabetes association. *Diabetes Care* **28**, 956–962
8. Callaghan, B. C., Little, A. A., Feldman, E. L., and Hughes, R. A. (2012) Enhanced glucose control for preventing and treating diabetic neuropathy. *Cochrane Database Syst. Rev.* CD007543
9. Vincent, A. M., Hinder, L. M., Pop-Busui, R., and Feldman, E. L. (2009) Hyperlipidemia: a new therapeutic target for diabetic neuropathy. *J. Peripher. Nerv. Syst.* **14**, 257–267
10. Wiggin, T. D., Sullivan, K. A., Pop-Busui, R., Amato, A., Sima, A. A., and Feldman, E. L. (2009) Elevated triglycerides correlate with progression of diabetic neuropathy. *Diabetes* **58**, 1634–1640
11. Vincent, A. M., Hayes, J. M., McLean, L. L., Vivekanandan-Giri, A., Pennathur, S., and Feldman, E. L. (2009) Dyslipidemia-induced neuropathy in mice: the role of oxLDL/LOX-1. *Diabetes* **58**, 2376–2385
12. Leinninger, G. M., Backus, C., Sastry, A. M., Yi, Y. B., Wang, C. W., and Feldman, E. L. (2006) Mitochondria in DRG neurons undergo hyperglycemic mediated injury through Bim, Bax and the fission protein Drp1. *Neurobiol. Dis.* **23**, 11–22
13. Vincent, A. M., Edwards, J. L., McLean, L. L., Hong, Y., Cerri, F., Lopez, I., Quattrini, A., and Feldman, E. L. (2010) Mitochondrial biogenesis and fission in axons in cell culture and animal models of diabetic neuropathy. *Acta Neuropathol.* **120**, 477–489
14. Vincent, A. M., Kato, K., McLean, L. L., Soules, M. E., and Feldman, E. L. (2008) Sensory neurons and Schwann cells respond to oxidative stress by increasing antioxidant defense mechanisms. *Antioxid. Redox Signal.* **11**, 425–438
15. Vincent, A. M., McLean, L. L., Backus, C., and Feldman, E. L. (2005) Short-term hyperglycemia produces oxidative damage and apoptosis in neurons. *FASEB J.* **19**, 638–640
16. Vincent, A. M., Russell, J. W., Low, P., and Feldman, E. L. (2004) Oxidative stress in the pathogenesis of diabetic neuropathy. *Endocr. Rev.* **25**, 612–628
17. Hinder, L. M., Vivekanandan-Giri, A., McLean, L. L., Pennathur, S., and Feldman, E. L. (2013) Decreased glycolytic and tricarboxylic acid cycle intermediates coincide with peripheral nervous system oxidative stress in a murine model of type 2 diabetes. *J. Endocrinol.* **216**, 1–11
18. Russell, J. W., Golovoy, D., Vincent, A. M., Mahendru, P., Olzmann, J. A., Mentzer, A., and Feldman, E. L. (2002) High glucose-induced oxidative stress and mitochondrial dysfunction in neurons. *FASEB J.* **16**, 1738–1748
19. Russell, J. W., Gong, C., Vincent, A., Berent, A. R., Mentzer, L. E., and Brownlee, M. (2001) Nitric oxide (NO) and mitochondrial manganese superoxide dismutase (MnSOD) regulate glucose-induced oxidative stress and programmed cell death in neurons. *Neurology* **56** (Suppl 3), A394
20. Pekkurnaz, G., Trinidad, J. C., Wang, X., Kong, D., and Schwarz, T. L. (2014) Glucose regulates mitochondrial motility via Milton modification by O-GlcNAc transferase. *Cell* **158**, 54–68
21. Sheng, Z. H. (2014) Mitochondrial trafficking and anchoring in neurons: new insight and implications. *J. Cell Biol.* **204**, 1087–1098
22. Grienberger, C., and Konnerth, A. (2012) Imaging calcium in neurons. *Neuron* **73**, 862–885
23. Macaskill, A. F., Rinholm, J. E., Twelvetrees, A. E., Arancibia-Carcamo, I. L., Muir, J., Fransson, A., Aspenstrom, P., Attwell, D., and Kittler, J. T. (2009) Miro1 is a calcium sensor for glutamate receptor-dependent localization of mitochondria at synapses. *Neuron* **61**, 541–555
24. Fransson, S., Ruusala, A., and Aspenström, P. (2006) The atypical Rho GTPases Miro-1 and Miro-2 have essential roles in mitochondrial trafficking. *Biochem. Biophys. Res. Commun.* **344**, 500–510
25. Van Spronsen, M., Mikhaylova, M., Lipka, J., Schlager, M. A., van den Heuvel, D. J., Kuijpers, M., Wulf, P. S., Keijzer, N., Demmers, J., Kapitein, L. C., Jaarsma, D., Gerritsen, H. C., Akhmanova, A., and Hoogenraad, C. C. (2013) TRAK/Milton motor-adaptor proteins steer mitochondrial trafficking to axons and dendrites. *Neuron* **77**, 485–502
26. De Vos, K. J., Chapman, A. L., Tennant, M. E., Manser, C., Tudor, E. L., Lau, K. F., Brownlees, J., Ackerley, S., Shaw, P. J., McLoughlin, D. M., Shaw, C. E., Leigh, P. N., Miller, C. C. J., and Grierson, A. J. (2007) Familial amyotrophic lateral sclerosis-linked SOD1 mutants perturb fast axonal transport to reduce axonal mitochondria content. *Hum. Mol. Genet.* **16**, 2720–2728
27. Magrané, J., Cortez, C., Gan, W. B., and Manfredi, G. (2014) Abnormal mitochondrial transport and morphology are common pathological denominators in SOD1 and TDP43 ALS mouse models. *Hum. Mol. Genet.* **23**, 1413–1424
28. Wang, Z. X., Tan, L., and Yu, J. T. (2015) Axonal transport defects in Alzheimer's disease. *Mol. Neurobiol.* **51**, 1309–1321
29. Vincent, A. M., Russell, J. W., Sullivan, K. A., Backus, C., Hayes, J. M., McLean, L. L., and Feldman, E. L. (2007) SOD2 protects neurons from injury in cell culture and animal models of diabetic neuropathy. *Exp. Neurol.* **208**, 216–227
30. Kaether, C., Skehel, P., and Dotti, C. G. (2000) Axonal membrane proteins are transported in distinct carriers: a two-color video microscopy study in cultured hippocampal neurons. *Mol. Biol. Cell* **11**, 1213–1224
31. De Vos, K. J., Sable, J., Miller, K. E., and Sheetz, M. P. (2003) Expression of phosphatidylinositol (4,5) bisphosphate-specific pleckstrin homology domains alters direction but not the level of axonal transport of mitochondria. *Mol. Biol. Cell* **14**, 3636–3649
32. De Vos, K. J., and Sheetz, M. P. (2007) Visualization and quantification of mitochondrial dynamics in living animal cells. *Methods Cell Biol.* **80**, 627–682
33. Nguyen, L. H., Robinton, D. A., Seligson, M. T., Wu, L., Li, L., Rakheja, D., Comerford, S. A., Ramezani, S., Sun, X., Parikh, M. S., Yang, E. H., Powers, J. T., Shinoda, G., Shah, S. P., Hammer, R. E., Daley, G. Q., and Zhu, H. (2014) Lin28b is sufficient to drive liver cancer and necessary for its maintenance in murine models. *Cancer Cell* **26**, 248–261
34. Scaduto, R. C., Jr., and Grotyohann, L. W. (1999) Measurement of mitochondrial membrane potential using fluorescent rhodamine derivatives. *Biophys. J.* **76**, 469–477
35. Sas, K. M., Kayampilly, P., Byun, J., Nair, V., Hinder, L. M., Hur, J., Zhang, H., Lin, C., Qi, N. R., Michailidis, G., Groop, P. H., Nelson, R. G., Darshi, M., Sharma, K., Schelling, J. R., Sedor, J. R., Pop-Busui, R., Weinberg, J. M., Soleimanpour, S. A., Abcouwer, S. F., Gardner, T. W., Burant, C. F., Feldman, E. L., Kretzler, M., Brosius III, F. C., and Pennathur, S. (2016) Tissue-specific metabolic reprogramming drives nutrient flux in diabetic complications. *JCI Insight* **1**, e86976
36. Hinder, L. M., Figueroa-Romero, C., Pacut, C., Hong, Y., Vivekanandan-Giri, A., Pennathur, S., and Feldman, E. L. (2014) Long-chain acyl coenzyme A synthetase 1 overexpression in primary cultured Schwann cells prevents long chain fatty acid-induced oxidative stress and mitochondrial dysfunction. *Antioxid. Redox Signal.* **21**, 588–600
37. Park, S. W., Yi, J. H., Miranpuri, G., Satriotomo, I., Bowen, K., Resnick, D. K., and Vemuganti, R. (2007) Thiazolidinedione class of peroxisome proliferator-activated receptor gamma agonists prevents neuronal damage, motor dysfunction, myelin loss, neuropathic pain, and inflammation after spinal cord injury in adult rats. *J. Pharmacol. Exp. Ther.* **320**, 1002–1012
38. Cai, Q., Zakaria, H. M., Simone, A., and Sheng, Z. H. (2012) Spatial parkin translocation and degradation of damaged mitochondria via mitophagy in live cortical neurons. *Curr. Biol.* **22**, 545–552
39. Rintoul, G. L., and Reynolds, I. J. (2010) Mitochondrial trafficking and morphology in neuronal injury. *Biochim. Biophys. Acta* **1802**, 143–150
40. Tao, K., Matsuki, N., and Koyama, R. (2014) AMP-activated protein kinase mediates activity-dependent axon branching by recruiting mitochondria to axon. *Dev. Neurobiol.* **74**, 557–573
41. Wang, X., Winter, D., Ashrafi, G., Schlehe, J., Wong, Y. L., Selkoe, D., Rice, S., Steen, J., LaVoie, M. J., and Schwarz, T. L. (2011) PINK1 and Parkin target Miro for phosphorylation and degradation to arrest mitochondrial motility. *Cell* **147**, 893–906
42. Yamamoto, H., Morino, K., Mengistu, L., Ishibashi, T., Kiriyama, K., Ikami, T., and Maegawa, H. (2016) Amla enhances mitochondrial spare respiratory capacity by increasing mitochondrial biogenesis and antioxidant systems in a murine skeletal muscle cell line. *Oxid. Med. Cell. Longev.* **2016**, 1735841
43. Cai, Q., Davis, M. L., and Sheng, Z. H. (2011) Regulation of axonal mitochondrial transport and its impact on synaptic transmission. *Neurosci. Res.* **70**, 9–15
44. Hollenbeck, P. J., and Saxton, W. M. (2005) The axonal transport of mitochondria. *J. Cell Sci.* **118**, 5411–5419
45. Saxton, W. M., and Hollenbeck, P. J. (2012) The axonal transport of mitochondria. *J. Cell Sci.* **125**, 2095–2104
46. Schwarz, T. L. (2013) Mitochondrial trafficking in neurons. *Cold Spring Harb. Perspect. Biol.* **5**, a011304

47. Takihara, Y., Inatani, M., Eto, K., Inoue, T., Kreymerman, A., Miyake, S., Ueno, S., Nagaya, M., Nakanishi, A., Iwao, K., Takamura, Y., Sakamoto, H., Satoh, K., Kondo, M., Sakamoto, T., Goldberg, J. L., Nabekura, J., and Tanihara, H. (2015) In vivo imaging of axonal transport of mitochondria in the diseased and aged mammalian CNS. *Proc. Natl. Acad. Sci. USA* **112**, 10515–10520
48. Wang, X., and Schwarz, T. L. (2009) Imaging axonal transport of mitochondria. *Methods Enzymol.* **457**, 319–333
49. American Diabetes Association. (2006) Standards of medical care in diabetes: 2006 (published correction in *Diabetes Care* 2006;29:1192). *Diabetes Care* **29**(Suppl 1), S4–S42
50. Stewart, M. A., Sherman, W. R., and Anthony, S. (1966) Free sugars in alloxan diabetic rat nerve. *Biochem. Biophys. Res. Commun.* **22**, 4–91
51. Stumvoll, M., Nurjhan, N., Perriello, G., Dailey, G., and Gerich, J. E. (1995) Metabolic effects of metformin in non-insulin-dependent diabetes mellitus. *N. Engl. J. Med.* **333**, 550–554
52. Psychogios, N., Hau, D. D., Peng, J., Guo, A. C., Mandal, R., Bouatra, S., Sinelnikov, I., Krishnamurthy, R., Eisner, R., Gautam, B., Young, N., Xia, J., Knox, C., Dong, E., Huang, P., Hollander, Z., Pedersen, T. L., Smith, S. R., Bamforth, F., Greiner, R., McManus, B., Newman, J. W., Goodfriend, T., and Wishart, D. S. (2011) The human serum metabolome. *PLoS One* **6**, e16957
53. Eguchi, K., Manabe, I., Oishi-Tanaka, Y., Ohsugi, M., Kono, N., Ogata, F., Yagi, N., Ohto, U., Kimoto, M., Miyake, K., Tobe, K., Arai, H., Kadowaki, T., and Nagai, R. (2012) Saturated fatty acid and TLR signaling link β cell dysfunction and islet inflammation. *Cell Metab.* **15**, 518–533
54. Gao, D., Griffiths, H. R., and Bailey, C. J. (2009) Oleate protects against palmitate-induced insulin resistance in L6 myotubes. *Br. J. Nutr.* **102**, 1557–1563
55. Merrill, G. F., Kurth, E. J., Rasmussen, B. B., and Winder, W. W. (1998) Influence of malonyl-CoA and palmitate concentration on rate of palmitate oxidation in rat muscle. *J Appl Physiol (1985)* **85**, 1909–1914
56. Ruddock, M. W., Stein, A., Landaker, E., Park, J., Cooksey, R. C., McClain, D., and Patti, M. E. (2008) Saturated fatty acids inhibit hepatic insulin action by modulating insulin receptor expression and post-receptor signalling. *J. Biochem.* **144**, 599–607
57. Iyer, S. P., Akimoto, Y., and Hart, G. W. (2003) Identification and cloning of a novel family of coiled-coil domain proteins that interact with O-GlcNAc transferase. *J. Biol. Chem.* **278**, 5399–5409
58. Mishra, P., and Chan, D. C. (2016) Metabolic regulation of mitochondrial dynamics. *J. Cell Biol.* **212**, 379–387
59. Miller, K. E., and Sheetz, M. P. (2004) Axonal mitochondrial transport and potential are correlated. *J. Cell Sci.* **117**, 2791–2804
60. Chang, D. T., and Reynolds, I. J. (2006) Mitochondrial trafficking and morphology in healthy and injured neurons. *Prog. Neurobiol.* **80**, 241–268
61. Ashrafi, G., Schlehe, J. S., LaVoie, M. J., and Schwarz, T. L. (2014) Mitophagy of damaged mitochondria occurs locally in distal neuronal axons and requires PINK1 and Parkin. *J. Cell Biol.* **206**, 655–670
62. Fu, M. M., Nirschl, J. J., and Holzbaur, E. L. (2014) LC3 binding to the scaffolding protein JIP1 regulates processive dynein-driven transport of autophagosomes. *Dev. Cell* **29**, 577–590
63. Lovas, J. R., and Wang, X. (2013) The meaning of mitochondrial movement to a neuron's life. *Biochim. Biophys. Acta* **1833**, 184–194
64. Cai, Q., and Sheng, Z. H. (2009) Moving or stopping mitochondria: Miro as a traffic cop by sensing calcium. *Neuron* **61**, 493–496
65. Saotome, M., Safiulina, D., Szabadkai, G., Das, S., Fransson, A., Aspenstrom, P., Rizzuto, R., and Hajnóczky, G. (2008) Bidirectional Ca2+-dependent control of mitochondrial dynamics by the Miro GTPase. *Proc. Natl. Acad. Sci. USA* **105**, 20728–20733
66. Remizov, O., Jakubov, R., Düfer, M., Krippeit Drews, P., Drews, G., Waring, M., Brabant, G., Wienbergen, A., Rustenbeck, I., and Schöfl, C. (2003) Palmitate-induced Ca2+-signaling in pancreatic beta-cells. *Mol. Cell. Endocrinol.* **212**, 1–9
67. Huang, J. M., Xian, H., and Bacaner, M. (1992) Long-chain fatty acids activate calcium channels in ventricular myocytes. *Proc. Natl. Acad. Sci. USA* **89**, 6452–6456
68. Tian, Y., Corkey, R. F., Yaney, G. C., Goforth, P. B., Satin, L. S., and Moitoso de Vargas, L. (2008) Differential modulation of L-type calcium channel subunits by oleate. *Am. J. Physiol. Endocrinol. Metab.* **294**, E1178–E1186
69. Webster, W. A., and Beyak, M. J. (2013) The long chain fatty acid oleate activates mouse intestinal afferent nerves in vitro. *Can. J. Physiol. Pharmacol.* **91**, 375–379
70. Schnell, S., Schaefer, M., and Schöfl, C. (2007) Free fatty acids increase cytosolic free calcium and stimulate insulin secretion from beta-cells through activation of GPR40. *Mol. Cell. Endocrinol.* **263**, 173–180
71. Karki, P., Kurihara, T., Nakamachi, T., Watanabe, J., Asada, T., Oyoshi, T., Shioda, S., Yoshimura, M., Arita, K., and Miyata, A. (2015) Attenuation of inflammatory and neuropathic pain behaviors in mice through activation of free fatty acid receptor GPR40. *Mol. Pain* **11**, 6
72. Belosludtsev, K. N., and Mironova, G. D. (2012) The mirochondrial lipid palmitate/Ca2+-induced pore and its possible role in a degradation of nervous cells [in Russian]. *Patol. Fiziol. Eksp. Ter.* **3**, 20–32
73. Koshkin, V., Dai, F. F., Robson-Doucette, C. A., Chan, C. B., and Wheeler, M. B. (2008) Limited mitochondrial permeabilization is an early manifestation of palmitate-induced lipotoxicity in pancreatic beta-cells. *J. Biol. Chem.* **283**, 7936–7948
74. Xu, S., Nam, S. M., Kim, J. H., Das, R., Choi, S. K., Nguyen, T. T., Quan, X., Choi, S. J., Chung, C. H., Lee, E. Y., Lee, I. K., Wiederkehr, A., Wollheim, C. B., Cha, S. K., and Park, K. S. (2015) Palmitate induces ER calcium depletion and apoptosis in mouse podocytes subsequent to mitochondrial oxidative stress. *Cell Death Dis.* **6**, e1976
75. Peeraer, E., Van Lutsenborg, A., Verheyen, A., De Jongh, R., Nuydens, R., and Meert, T. F. (2011) Pharmacological evaluation of rat dorsal root ganglion neurons as an in vitro model for diabetic neuropathy. *J. Pain Res.* **4**, 55–65
76. Gumy, L. F., Bampton, E. T., and Tolkovsky, A. M. (2008) Hyperglycaemia inhibits Schwann cell proliferation and migration and restricts regeneration of axons and Schwann cells from adult murine DRG. *Mol. Cell. Neurosci.* **37**, 298–311
77. Zherebitskaya, E., Akude, E., Smith, D. R., and Fernyhough, P. (2009) Development of selective axonopathy in adult sensory neurons isolated from diabetic rats: role of glucose-induced oxidative stress. *Diabetes* **58**, 1356–1364
78. Malin, S. A., Davis, B. M., and Molliver, D. C. (2007) Production of dissociated sensory neuron cultures and considerations for their use in studying neuronal function and plasticity. *Nat. Protoc.* **2**, 152–160
79. Vincent, A. M., Olzmann, J. A., Brownlee, M., Sivitz, W. I., and Russell, J. W. (2004) Uncoupling proteins prevent glucose-induced neuronal oxidative stress and programmed cell death. *Diabetes* **53**, 726–734
80. Akude, E., Zherebitskaya, E., Chowdhury, S. K., Smith, D. R., Dobrowsky, R. T., and Fernyhough, P. (2011) Diminished superoxide generation is associated with respiratory chain dysfunction and changes in the mitochondrial proteome of sensory neurons from diabetic rats. *Diabetes* **60**, 288–297
81. Sharma, K. (2015) Mitochondrial hormesis and diabetic complications. *Diabetes* **64**, 663–672
82. Ho, P. W., Ho, J. W., Liu, H. F., So, D. H., Tse, Z. H., Chan, K. H., Ramsden, D. B., and Ho, S. L. (2012) Mitochondrial neuronal uncoupling proteins: a target for potential disease-modification in Parkinson's disease. *Transl. Neurodegener.* **1**, 3
83. Callaghan, B. C., Hur, J., and Feldman, E. L. (2012) Diabetic neuropathy: one disease or two? *Curr. Opin. Neurol.* **25**, 536–541

Received for publication March 10, 2017.
Accepted for publication August 21, 2017.